

High pressure sequence of $\text{Ba}_3\text{NiSb}_2\text{O}_9$ structural phases: new $S = 1$ quantum spin-liquids based on Ni^{2+}

J. G. Cheng,¹ G. Li,² L. Balicas,² J. S. Zhou,¹ J. B. Goodenough,¹ Cenke Xu,³ and H. D. Zhou^{2,*}

¹*Texas Materials Institute, University of Texas at Austin, TX 78712, USA*

²*National High Magnetic Field Laboratory, Florida State University, Tallahassee, FL 32306-4005, USA*

³*Department of Physics, University of California, Santa Barbara, California 93106, USA*

(Dated: August 16, 2011)

By using a high pressure, high temperature (HPHT) technique, the antiferromagnetically ordered ($T_N = 13.5$ K) 6H-A phase of $\text{Ba}_3\text{NiSb}_2\text{O}_9$ was transformed into two new gapless quantum spin liquid (QSL) candidates with $S = 1$ (Ni^{2+}) moments: the 6H-B phase with a Ni^{2+} -triangular lattice and the 3C-phase with a Ni^{2+} -three-dimensional (3D) edge-shared tetrahedral lattice. Both compounds show no magnetic order down to 0.35 K despite Curie-Weiss temperatures θ_{CW} of -75.5 K (6H-B) and -182.5 K (3C), respectively. Below ~ 25 K the magnetic susceptibility of the 6H-B phase saturates to a constant value $\chi_0 = 0.013$ emu/mol which is followed below 7 K, by a linear-temperature dependent magnetic specific heat (C_M) displaying a giant coefficient $\gamma = 168$ mJ/mol-K². Both observations suggest the development of a Fermi-liquid like ground state characterized by a Wilson ratio of 5.6 in this insulating material. For the 3C phase, the $C_M \propto T^2$ behavior indicates a unique $S = 1$, 3D QSL ground-state.

PACS numbers: 75.40.Cx, 75.45.+j, 61.05.C-

A quantum spin-liquid (QSL) is a ground-state where strong quantum-mechanical fluctuations prevent a phase-transition towards conventional magnetic order and make the spin ensemble to remain in a liquid-like state [1, 2]. So far various gapped spin liquids have been found in dimerized spin systems and spin ladders [3–10]. However, topological and gapless spin liquids are much less well-understood in dimensions higher than one. Most of the gapless QSL candidates studied to date are two-dimensional frustrated magnets composed of either a triangular lattice of $S = 1/2$ dimers, such as the organic compounds κ -(BEDT-TTF)₂Cu₂(CN)₃[11, 12] (abbreviated as ET) or EtMe₃Sb[Pd(dmit)₂]₂[13, 14] (abbreviated as dmit), or of a kagome lattice of Cu^{2+} ($S = 1/2$) ions, such as the $\text{ZnCu}_3(\text{OH})_6\text{Cl}_2$ [15, 16], $\text{BaCu}_3\text{V}_2\text{O}_8(\text{OH})_2$ [17], and the $\text{Cu}_3\text{V}_2\text{O}_7(\text{OH})_2 \cdot 2\text{H}_2\text{O}$ [18] compounds.

However, whether a gapless QSL can be realized in systems with larger spins, e.g. $S = 1$, especially in systems with a three-dimensional (3D) lattice, is still a matter of debate. For example, the $S = 1$ material NiGa_2S_4 [19] with a triangular lattice develops quadrupolar order [20, 21], while so far all the 3D gapless QSL candidates studied to date, such as $\text{Na}_3\text{Ir}_4\text{O}_8$ with Ir^{4+} ions [22], are either $S = 1/2$ or effective $S = 1/2$ systems due to strong spin-orbit coupling. Therefore, the present challenge is to find additional model compounds to test current theories for gapless QSLs. The key to find a new QSL candidate is to construct a geometrically frustrated lattice with specific magnetic ions. A commonly used method to design and discover new materials is to pursue chemical substitutions, although the application of high pressures is also an alternative way to transform crystalline structures and discover new phases which has not been widely

used for synthesizing new frustrated magnets. Here, we followed the second route to synthesize frustrated magnets $\text{Ba}_3\text{NiSb}_2\text{O}_9$ displaying the unique physical properties shown below.

The ambient pressure 6H-A phase of $\text{Ba}_3\text{NiSb}_2\text{O}_9$ was synthesized through a conventional solid-state reaction. Its x-ray diffraction (XRD) pattern (recorded at room temperature with Cu K_α radiation, Fig. 1(a)) shows a single phase having the hexagonal space group $P6_3/\text{mmc}$. The obtained lattice parameters $a = 5.8376(5)$ Å and $c = 14.4013(1)$ Å agree well with previously reported values [23, 24]. The structure of the 6H-A phase (Fig. 1(d)) consists of dimers of face-sharing Sb_2O_9 octahedra linked by their vertices to single corner-sharing $\text{NiO}_{6/2}$ octahedra along the c axis. The Ni^{2+} ions occupy the 2a Wyckoff site to form a two-dimensional (2D) triangular lattice in the ab plane (Fig. 1(g)), which is separated by two non-magnetic Sb layers.

The 6H-B phase of $\text{Ba}_3\text{NiSb}_2\text{O}_9$ was obtained by treating the 6H-A phase at 600 °C under a pressure of 3 GPa for 1 hour in a Walker-type multianvil module (Rockland Research Co.). Its XRD pattern (Fig. 1(b)) is different from that of 6H-A phase and can be satisfactorily indexed as a distinct hexagonal space group, i.e. the $P6_3\text{mc}$ with $a = 5.7923(2)$ Å and $c = 14.2922(7)$ Å, respectively. In this structure (Fig. 1(e)), the dimers of the face-sharing NiSbO_9 octahedra (instead of the Sb_2O_9 octahedra as for the 6H-A phase) are linked by their vertices to single corner-sharing $\text{SbO}_{6/2}$ octahedra along the c axis. In the well ordered NiSbO_9 octahedra, the Ni^{2+} ions occupy the 2b Wyckoff sites, which still form a triangular lattice in the ab plane. For the 6H-A phase, the layers of the Ni triangular lattice are exactly on top of each other along the c -axis. However, for the 6H-B phase, the nearest two lay-

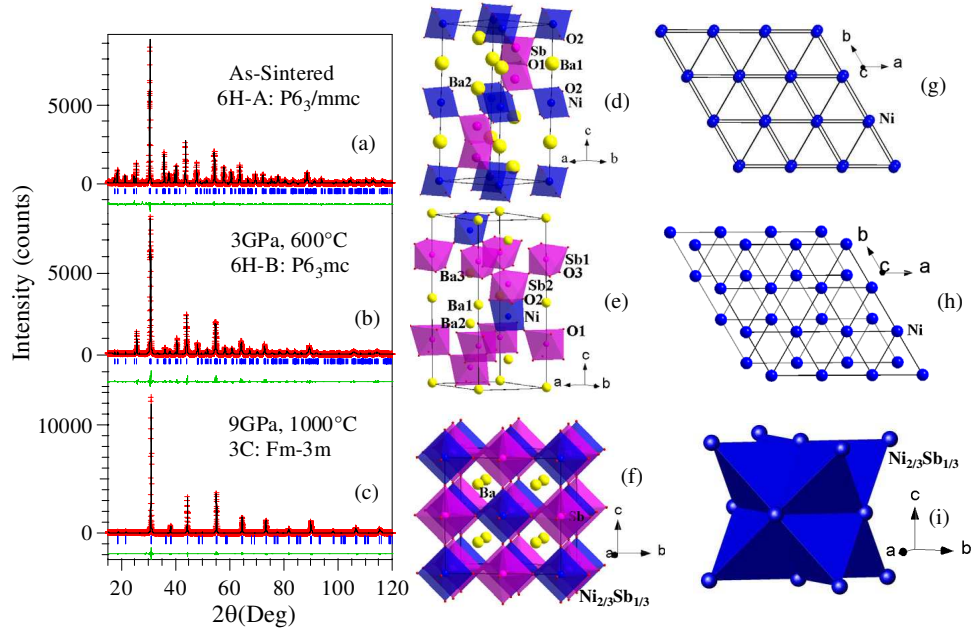


FIG. 1: (Color online) Powder XRD patterns (crosses) at 295 K for the $\text{Ba}_3\text{NiSb}_2\text{O}_9$ polytypes: (a) 6H-A, (b) 6H-B, and (c) 3C. Solid curves are the best fits obtained from Rietveld refinements using FullProf. Schematic crystal structures for the $\text{Ba}_3\text{NiSb}_2\text{O}_9$ polytypes: (d) 6H-A, (e) 6H-B, and (f) 3C, red octahedra represents $\text{Sb}(\text{M}')$ site and blue octahedra represents $\text{Ni}_{2/3}\text{Sb}_{1/3}(\text{M})$ site. Magnetic lattices composed of Ni^{2+} ions for the $\text{Ba}_3\text{NiSb}_2\text{O}_9$ polytypes: (g) 6H-A, (h) 6H-B, and (i) 3C.

ers of the Ni triangular lattice are displaced with respect to each other in a way that the Ni ion in one layer is projected towards the center of the triangle formed by the Ni ions in the adjacent layers along the c -axis, as shown in Fig. 1(h). The instability of the 6H-A phase should arise from the fact that high pressures tend to reduce the $\text{Sb}^{5+}\text{-Sb}^{5+}$ distance and therefore partially relieve strong electrostatic repulsion by exchanging Ni with one of the Sb atoms. Battle *et al.* reported a similar structure for the 6H-B phase [25], but with no physical characterization.

With increasing pressure we observed an additional phase transformation to a cubic perovskite structure. This 3C phase was obtained under 9 GPa and at a temperature of 1000 °C kept for 30 min. Its XRD pattern (Fig. 1(c)) is best described as a double-perovskite in a $\text{Ba}_2\text{MM}'\text{O}_6$ model with the cubic space group Fm-3m having a lattice parameter $a = 8.1552(2)$ Å. The refinement shows a full-ordered arrangement of $\text{Ni}_{2/3}\text{Sb}_{1/3}$ and Sb atoms at the M and M' sites (Fig. 1(f)), respectively. Therefore the $\text{Ni}_{2/3}\text{Sb}_{1/3}$ sites form a network of edge-shared tetrahedra, as shown in Fig. 1(i). Instead of adopting a primitive perovskite structure in which the Ni^{2+} and Sb^{5+} ions are randomly distributed, the preferred double-perovskite structure should be attributed to the large difference in charges between the Ni^{2+} and the Sb^{5+} ions.

All three samples are insulators with the room temperature resistance higher than 20 MΩ. The DC magnetic

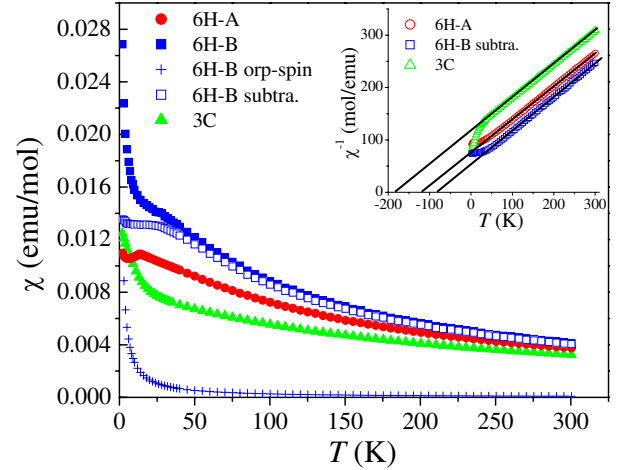


FIG. 2: (Color online) (a) Temperature dependencies of the DC magnetic susceptibility (χ) for the $\text{Ba}_3\text{NiSb}_2\text{O}_9$ polytypes. Inset: Temperature dependencies of $1/\chi$. The solid lines on $1/\chi$ data represent Curie-Weiss fits. For 6H-B phase, χ (open squares) is obtained by subtracting 1.7% Ni^{2+} orphan spin's contribution (crosses) from the as measured data (solid squares).

susceptibility ($\chi(T)$, Fig. 2) for all three compounds was measured under a field $H = 5000$ Oe. For each compound, one does not observe any difference between the data measured under zero-field-cooled (ZFC) and that

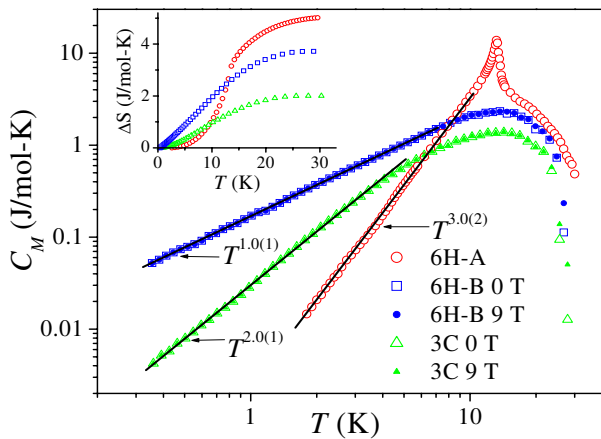


FIG. 3: (Color online) (a) Temperature dependencies for the magnetic specific heat (C_M) for all three $\text{Ba}_3\text{NiSb}_2\text{O}_9$ polytypes. Solid lines are the fits as described in the main text. Inset: variation in magnetic entropy ΔS below 30 K.

measured under field-cooled (FC) conditions. The 6H-A sample exhibits a cusp-like anomaly at the antiferromagnetic ordering temperature $T_N = 13.5$ K, as previously reported [24]. On the other hand, neither the 6H-B nor the 3C phase show any sign of long range magnetic order down to 2 K. For the 6H-B phase, we have subtracted the Curie contribution provided by 1.7 % Ni^{2+} of orphan spins from the as measured data. This percentage of Ni^{2+} orphan spins was calculated from fitting the specific heat data [26]. After this subtraction, $\chi(T)$ for the 6H-B phase (open squares in Fig. 2) basically saturates below 25 K with a saturation value $\chi_0 \sim 0.013$ emu/mol. The fittings of the high-temperature region of $\chi^{-1}(T)$ to the Curie-Weiss law show that all three compounds have the same value for effective moment, $\mu_{\text{eff}} \sim 3.54 \mu_B$, as seen from the fact that all three $\chi^{-1}(T)$ curves are basically parallel to each other (insert of Fig. 2). This value gives a g-factor of 2.5, which is close to the typical value for Ni^{2+} ions with spin-orbital coupling [27]. The Curie-Weiss temperatures, θ_{CW} , obtained for the 6H-A, 6H-B, and 3C phases are -116.9(4) K, -75.6(6) K, and -182.5(3) K, respectively, indicating dominant antiferromagnetic interactions for all compounds.

The magnetic specific-heat (C_M , Fig. 3) for each compound was obtained by subtracting the heat capacity of the non-magnetic compound $\text{Ba}_3\text{ZnSb}_2\text{O}_9$ ordered in the 6H-A, 6H-B, and 3C phases, respectively, which are used here as lattice standards. For the 6H-B phase a Schottky anomaly due to 1.7% of Ni^{2+} orphan spins was also subtracted, see Supplemental Materials [26]. For the 6H-A phase, C_M shows a sharp peak around $T_N = 13.5$ K. On the other hand, for both the 6H-B and the 3C phases, C_M which emerges from around 30 K, shows a broad peak around 13 K with no sign for long-range magnetic-order down to $T = 0.35$ K. For the 6H-B and the 3C

phases, C_M is not at all affected by the application of a magnetic field as large as $H = 9$ T. Below 30 K, the associated change in magnetic entropy (inset of Fig. 3) is 5.0 J/mol-K, 3.7 J/mol-K, and 2.0 J/mol-K for the 6H-A, 6H-B, and the 3C phase, respectively. These values correspond respectively, to 55%, 41%, and 22% of $R \ln(3)$ for a $S = 1$ system, where R is the gas constant. The remarkable result is that C_M at low temperatures for all three phases follows a γT^α behavior, but with a distinct value of α for each phase. As shown in Fig. 3, a linear fit of C_M plotted in a log-log scale yields respectively, $\gamma = 2.0(1)$ mJ/mol-K⁴ and $\alpha = 3.0(2)$ for the 6H-A phase in the range $1.8 \leq T \leq 10$ K, $\gamma = 168(3)$ mJ/mol-K² with $\alpha = 1.0(1)$ for the 6H-B phase when $0.35 \leq T \leq 7$ K, and $\gamma = 30(2)$ mJ/mol-K³ with $\alpha = 2.0(1)$ for 3C phase within $0.35 \leq T \leq 5$ K.

Both the susceptibility and the specific heat show no evidence for magnetic ordering down to $T = 0.35$ K for either the 6H-B or the 3C phase, despite moderately strong antiferromagnetic interactions. The 41% (6H-B) and the 22% (3C) change in magnetic entropy also indicates a high degeneracy of low-energy states at low temperatures. These behaviors suggest that both the 6H-B and 3C phases are candidates for spin liquid behavior. For the 6H-A phase, the $C_M \propto T^3$ behavior observed below T_N is typical for 3D magnons [28]. This indicates that besides the intra-layer magnetic interactions within the Ni^{2+} triangular lattice, the inter-layer coupling is also relevant for this phase. As for the 6H-B phase, on the other hand, the relative shift of the two nearest Ni^{2+} triangular layers leads to a frustrated inter-layer magnetic coupling, which prevents 3D long-range magnetic-order. The linear- T dependent C_M of the 6H-B phase is unusual for a magnetic insulator having a 2D frustrated lattice. Naively, for a 2D lattice one would expect C_M to display a T^2 dependence given by a linearly dispersive low-energy mode [19].

In fact, a series of recent low temperature studies reveal that $C_M \propto \gamma T$, with a considerable large value for γ , is a common feature among QSL candidates [11, 29, 30]. For example, ET[11], dmit[29], and $\text{Ba}_3\text{CuSb}_2\text{O}_9$ [30], all composed of a $S = 1/2$ triangular lattice, display $\gamma = 12.0$ mJ/mol-K², 19.9 mJ/mol-K², and 43.4 mJ/mol-K², respectively. It has been proposed theoretically that magnetic excitations or quasiparticles called spinons can lead to a Fermi surface even in a Mott insulator, which yields a linear term in the specific heat after the $U(1)$ gauge fluctuation is suppressed due to partial pairing on the fermi surface [31]. The observation of a saturation in $\chi(T)$ for 6H-B phase enables us to calculate the Wilson ratio, $R_W = [4\pi^2 k_B^2 \chi_0] / [3(g\mu_B)^2 \gamma]$. One obtains a value of 5.6 by using $\chi_0 = 0.013$ emu/mol and $\gamma = 168$ mJ/mol-K². In metals, a Pauli-like paramagnetic susceptibility and a linear- T dependent heat capacity, as seen for the 6H-B phase at lower temperatures, which leads to a concomitant R_W in the order of unity, are conven-

tional properties of Fermi-liquids. Therefore, we are lead to conclude that coherent fermionic like excitations or quasiparticles, which in an insulator can only be magnetic in nature such as the spinons, are responsible for the low temperature behavior of the 6H-B phase.

It is known that the ground state of quantum $S = 1$ magnets depends on the detailed competition between Heisenberg and biquadratic spin couplings [20, 21]. Therefore, although NiGa_2S_4 and the 6H-B phase both have similar triangular lattice structure and spin-1 on each site, their ground states can be very different. The ground state of NiGa_2S_4 has quadrupolar order [20, 21] with $C_M \propto T^2$, while in $\text{Ba}_3\text{NiSb}_2\text{O}_9$ we believe it is the spinon fermi surface that leads to the constant χ and γ at zero temperature.

For the 3C phase, despite diluting non-magnetic Sb^{5+} ions on the Ni sites, the magnetic interactions between Ni^{2+} ions are still moderately strong indicated by a $\theta_{\text{CW}} = -182.5$ K. The spin liquid like ground-state then is possibly led by the geometrically frustrated edge-shared tetrahedra composed of $\text{Ni}_{2/3}\text{Sb}_{1/3}$ sites. The 3C phase crystallizes in a 3D instead of a 2D lattice, and therefore the T^2 dependence observed for C_M is also unconventional. $\text{Na}_4\text{Ir}_3\text{O}_8$, with a 3D $S = 1/2$ (Ir^{4+}) hyperkagome lattice [22], also displays a $C_M \propto T^2$ behavior at low T s, which is claimed to be strong evidence for a QSL ground state and is explained in terms of a spinon Fermi-surface which is unstable against a spinon pairing state with line nodes at low energies[32]. A similar scenario could be pertinent for the 3C phase with a face centered cubic structure in which the nearest-neighbour exchange interaction J_1 between the $[000]$ and $[1/2, 1/2, 0]$ spins on the network of edge-sharing tetrahedra, is the dominant interaction with a second-neighbour exchange interaction J_2 along the $[100]$ wave-vector being the weaker one. Former studies on the double-perovskite $\text{Ba}_2\text{MM}'\text{O}_6$ already showed that the competition between J_1 and J_2 can lead to interesting frustrated magnetic ground states, such as the valence bond glass state in Ba_2YMoO_6 [33].

Gapless QSLs are claimed to exist in 3D lattices, or be composed of spins larger than $S = 1/2$. For instance, for spin- S systems, the spin model can be tuned to a $\text{SU}(2S+1)$ invariant point, where quantum fluctuation is significantly enhanced, and the semiclassical spin order is suppressed. Here, we revealed two unique QSL candidates: (i) the 6H-B phase of $\text{Ba}_3\text{NiSb}_2\text{O}_9$ having a $S = 1$ moment on a triangular lattice and displaying $C_M \propto \gamma T$ with a giant $\gamma = 168$ mJ/mol-K², therefore suggesting the realization of a ground state with a possible spinon fermi surface but on a $S = 1$ system; and (ii) the 3C phase of $\text{Ba}_3\text{NiSb}_2\text{O}_9$ with a edge-shared tetrahedral lattice, displaying $C_M \propto \gamma T^2$, thus suggesting a rare example of a 3D-QSL composed of $S = 1$ moments.

Most importantly, we proved that quantum fluctuations are also particularly relevant for $S = 1$ geometrically frustrated systems, which are observed to follow physical behavior either predicted for or observed in geometrically frustrated systems composed of $S = 1/2$ moments.

We acknowledge P. A. Lee for discussions, and the critical reading of this manuscript. This work was supported by NSF (DMR 0904282, CBET 1048767) and the Robert A Welch foundation (Grant F-1066). The NHMFL and therefore H.D.Z. is supported by NSF-DMR-0654118 and the State of Florida. L.B. is also supported by DOE-BES through award de-sc0002613.

* Electronic address: zhou@magnet.fsu.edu

- [1] L. Balents, *Nature* **464**, 199 (2010).
- [2] R. Moessner and A. P. Ramirez, *Physics Today* **59**, 24 (2006).
- [3] Ch. Rüegg *et al.*, *Phys. Rev. Lett.* **95**, 267201 (2005).
- [4] Ch. Rüegg *et al.*, *Phys. Rev. Lett.* **101**, 247202 (2008).
- [5] S. H. Lee *et al.*, *J. Phys. Soc. Jpn.* **79**, 011004 (2010).
- [6] G. Y. Xu *et al.*, *Phys. Rev. Lett.* **84**, 4465 (2000).
- [7] M. Kenzelmann *et al.*, *Phys. Rev. Lett.* **90**, 087202 (2003).
- [8] T. Hong *et al.*, *Phys. Rev. Lett.* **105**, 137207 (2010).
- [9] B. D. Gaulin *et al.*, *Phys. Rev. Lett.* **93**, 267202 (2004).
- [10] J. S. Gardner *et al.*, *Phys. Rev. Lett.* **82**, 1012 (1999).
- [11] S. Yamashita *et al.*, *Nature Phys.* **4**, 459 (2008).
- [12] M. Yamashita *et al.*, *Nature Phys.* **5**, 44 (2009).
- [13] M. Yamashita *et al.*, *Science* **328**, 1246 (2010).
- [14] T. Itou *et al.*, *Nature Phys.* DOI:10.1038/nphys1715.
- [15] J. S. Helton *et al.*, *Phys. Rev. Lett.* **98**, 107204 (2007).
- [16] S. H. Lee *et al.*, *Nature Mater.* **6**, 853 (2007).
- [17] Y. Okamoto *et al.*, *J. Phys. Soc. Jpn.* **78**, 033701 (2009).
- [18] Z. Hiroi *et al.*, *J. Phys. Soc. Jpn.* **70**, 3377 (2001).
- [19] S. Nakatsuji *et al.*, *Science* **309**, 1697 (2005).
- [20] E. M. Stoudenmire *et al.*, *Phys. Rev. B* **79**, 214436 (2009).
- [21] Subhro Bhattacharjee *et al.*, *Phys. Rev. B* **74**, 092406 (2009).
- [22] Y. Okamoto *et al.*, *Phys. Rev. Lett.* **99**, 137207 (2007).
- [23] Von. U. Treiber *et al.*, *Z. Anorg. Allg. Chem.* **487**, 161 (1982).
- [24] Y. Doi *et al.*, *J. Phys.: Condens. Matter* **16**, 8923 (2004).
- [25] P. D. Battle *et al.*, *J. Solid State Chem.* **85**, 144 (1990).
- [26] see Supplemental Materials at.
- [27] R. L. Carlin, *Magnetochemistry* (Berlin: Springer) chapter 4 (1986).
- [28] J. A. Gotaas *et al.*, *Phys. Rev. B* **32**, 4519 (1985).
- [29] S. Yamashita *et al.*, *Nature Commun.* DOI:10.1038/ncomms1274.
- [30] H. D. Zhou *et al.*, *Phys. Rev. Lett.* **106**, 147204 (2011).
- [31] S. S. Lee *et al.*, *Phys. Rev. Lett.* **98**, 067006 (2007).
- [32] M. J. Lawler *et al.*, *Phys. Rev. Lett.* **101**, 197202 (2008).
- [33] M. A. Vries *et al.*, *Phys. Rev. Lett.* **104**, 177202 (2010).